A R C H I V E S O F M E T A L L U R G Y A N D M A T E R I A L S
Volume 50 2005 Issue 4

M. SUŁOWSKI*

NITROGEN AS AN ALTERNATIVE SINTERING ATMOSPHERE FOR PRODUCTION OF PM PARTS

AZOT JAKO ALTERNATYWNA ATMOSFERA STOSOWANA DO PRODUKCJI SPIEKANYCH STALI KONSTRUKCYJNYCH

The improvements in powder metallurgy (PM) Ni-free structural steels technology seem modest, but they resulted in a substantial improvement in quality and consistency of the material. This has been especially significant in the case of the Mn steels where marked improvements in strength and toughness have been achieved. These have mostly resulted from a better control of reactions between the sintered steel and furnace atmosphere during the whole sintering cycle, and better identification of microstructural features that are critical to the properties of PM Mn steels.

The main problem, which has been coped with for years, is that the manganese oxide network forms in the conventionally sintered compacts and imparts brittleness to the as-sintered material. It has been found that sintering in semi-closed containers offers an excellent solution, whereby better mechanical properties and dimensional accuracy can be achieved. It is also important that the reducing atmosphere (hydrogen or dissociated ammonia) can be replaced with cheaper nitrogen with negligible effects on the properties of sintered steels.

To show the alternative way of production PM sintered parts, single compacted specimens with green density approx. 6.9 g/cm^3 were isothermal sintered at 1220°C in nitrogen and hydrogen atmospheres. Because of "sinter-hardening" effect, the specimens were subsequently tempered at 200°C. As- sintered and tempered density was approx. 6.9 g/cm^3. Investigations were carried out on "dogbone" ISO 2740 bars. Following strength tests apparent and cross-sectional hardness was calculated. To examine the structure, optical microscopy was employed.

In this paper the possibility of sintering Fe-(Mn)-(Mo)-C steels in differ than hydrogen atmosphere is discussed.

Keywords: Mn PM steels, (Mn)-(Mo) PM steels, alloying elements, sintering, high sintering temperature, sinter-hardening, tempering.

* WYDZIAŁ METALURGII I INŻYNIERII MATERIAŁOWEJ, AKADEMIA GÓRNICZO-HUTNICZA, 30-059 KRAKÓW, AL. MICKIEWICZA 30

Niewielkie zmiany wprowadzone w technologii wytwarzania spiekanych bezniklowych stali konstrukcyjnych przyczyniły się do znacznej poprawy ich własności wytrzymałościowych. Głównym problemem pojawiającym się podczas spiekania tych stali jest utrzymanie założonego punktu rosy atmosfery spiekania. Niespełnienie tego warunku jest powodem do powstawania siatki tlenków na granicy ziarn, czego skutkiem jest znaczne obniżenie własności mechanicznych spieków. Zastosowanie podczas spiekania specjalnej zasypki lub prowadzenie procesu w półhermetycznej łódce pozwala zminimalizować to niekorzystne zjawisko i przyczynia się do wzrostu własności oraz zachowania stabilności wymiarowej spiekanych elementów.

Dotychczasowa produkcja spiekanych stali manganowych prowadzona była najczęściej w atmosferze wodoru lub zdysocjowanego amoniaku. W przypadku zastosowania tańszej atmosfery azotowej własności mechaniczne otrzymanych spieków były porównywalne z własnościami spieków wytwarzanymi w atmosferze redukującej.

W celu pokazania alternatywnego sposobu produkcji spiekanych materiałów konstrukcyjnych, jednokrotnie sprasowane kształtki o gęstości około 6,9 g/cm^3 poddano spiekaniu w temperaturze 1220°C w atmosferze azotu oraz wodoru, a następnie odpuszczano w temperaturze 200°C. Badania struktury i własności mechanicznych spiekanych stali przeprowadzono na próbkach wykonanych zgodnie z PN-EN ISO 2740.

W artykule przedstawiono możliwość zastosowania atmosfery azotu od produkcji spiekanych manganowych stali konstrukcyjnych z dodatkiem molibdenu.

1. Introduction

Sintered PM steels based on iron and ferroalloys used to be produce in laboratory and industrial conditions in hydrogen or hydrogen-rich atmospheres. This point of view was represented by most of researchers. The main reason to use hydrogen-based atmospheres was its oxide reduction properties in Fe-Metal-O system. Mixture of powders contain manganese, added in metallic of ferroalloy forms, had to be sinter in a protective atmosphere, because of high affinity of manganese to the oxygen. In 90's this point of view had changed, when from investigations were concluded, that there is a possibility of production PM manganese containing sintered parts in semi-closed container or in a special getter. Last few years brought the progress in fabrication this group of steels. It was found out that it is possible to use nitrogen as a cheap and safe atmosphere to produce PM manganese containing steels [1].

Also the strengthening effect of small addition of manganese in PM steels is being recognised. Manganese is the one of the cheapest alloying element increases mechanical properties of steels. As nickel is expensive and cancerogenic element, subsiding Mn for Ni was the interest of PM manufacturers. Also in terms of cost effectiveness, the advantage of manganese over nickel is clear [2, 3].

Molybdenum is being recognised as one of the important elements in ferrous powder metallurgy. The beneficial effect of this alloying element on the properties of PM steels can be explained by the solid solution hardening. Addition of molybdenum in PM steels increasing their tensile strength and hardenability without decreasing the ductility. So then the combined effect of Mn and Mo in sintered steels may often be important than the specific effect of each other [4-6].

Nowadays sintered Fe-(Mn)-(Mo)-(Cr)-C steels are still being now the interest of powder metallurgist from all over the world. The effect of both Mn and Mo addition was deeply examined by Wronski et al., Mitchell et al., Keresti et al., Youseffi et al. and Salak et al. [7-11].

2. Experimental procedure

Base powders

Six PM steels based on Höganäs NC 100.24 sponge iron powder (Fig. 1a) were manufactured and examined. The manganese was added in the form of ferromanganese powders. Tree types of ferromanganese powders were used: low-carbon, low-silicon (1.3 wt.-% of C, 77 wt.-% of Mn) medium-carbon high-silicon (3.67 wt.-% of C, 8.84 wt.-% of Si, 61 wt.-% of Mn) and high-carbon, low-silicon (6.25 wt.-% of C, 0.71 wt.-% of Si, 73 wt.-% of Mn). The first ferromanganese powder (table 1) was provided as a fine powder by Huta Baildon (Fig. 1b), having nominal particle size as measured by sedimentation method 12 μm. The second and the third one were produced in ZM "Trzebinia" and were milled in nitrogen atmosphere (Fig. 1c).

TABLE 1

Chemical composition of based powders

Powder	Chemical composition, wt.-%					
	Fe	Mn	C	Si	O	S
NC 100.24	99.78	—	<0.01	—	0.21	—
Elkem	bal.	76.96	1.30	—	2.28	—
HP I	bal.	61.37	3.67	8.84	1.62	0.001
HP II	bal.	72.77	6.26	0.71	1.29	0.0032

Molybdenum was introduced in the form of prealloyed Höganäs Astaloy Mo powder (1.5 wt.-% of Mo) (Fig. 1d). Elemental carbon was added to powders' mixtures in the form of ultra fine graphite (Höganäs C-UF - Fig. 1e).

Mixing

Mixtures of powders with different manganese and carbon content and constant molybdenum concentration (table 2) were prepared by blending base powders in a double cone laboratory mixer (60 min, 50 rev./min) to produce mixtures of the required uniform particles distribution. No lubricant was added to the powders before mixing.

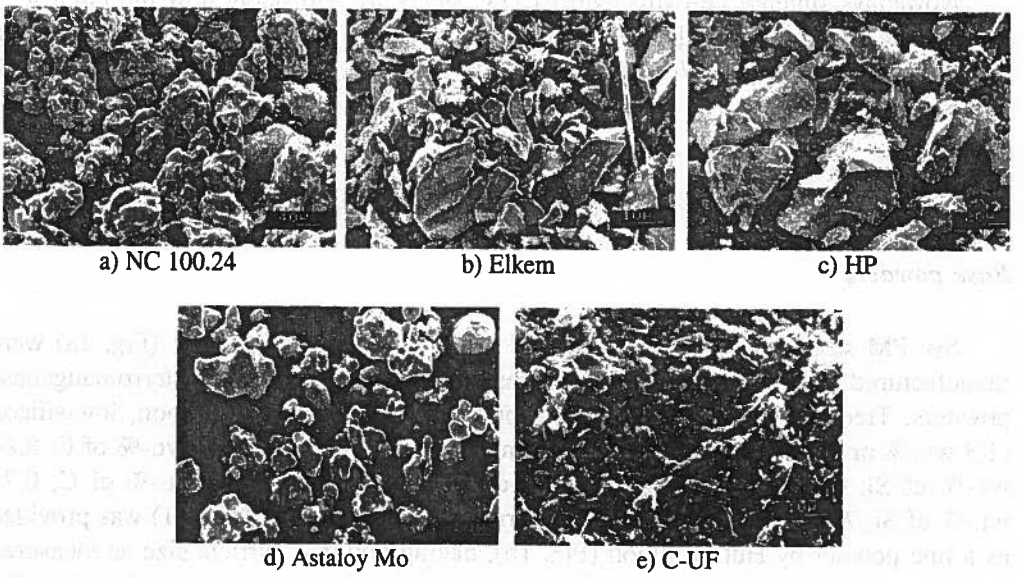

Fig. 1. Microphotographs of base powders: (a) sponge iron powder grade NC 100.24, (b) Elkem ferromanganese powder, (c) HP ferromanganese powder, (d) Astaloy Mo prealloyed powder and (e) C-UF graphite powder

Compacting

The blended powders were compacted in steel die with zinc stearate lubricated walls. Unaxial, single-action compacting with a stationary lower punch was used. Tensile strength test bars were pressed under pressure of 660 MPa. Dogbone tensile test bars were prepared according to ISO 2740 standard.

Sintering

Sintering was carried out in dry hydrogen and nitrogen atmospheres in a horizontal laboratory furnace. The heat resisting steel tube furnace was equipped with water jacketed rapid convective cooling zone. The dew point of the sintering atmospheres was –60°C (15 ppm moisture). Compacts were heated to the sintering temperature at heating rate of 75°C/min. The temperature control was ± 2°C. Sintering was performed at 1220°C for 60 minutes employing rapid (convective) cooling. The convective cooling rate, determined in the temperature range of 1100÷500°C, was approximately 64°C/min. To improve both the local dew point (self-gettering effect) and to minimise the loss of manganese and molybdenum due to volatilisation, the specimens were sintered in a semi- closed stainless steel container. After sintering, all the specimens

were tempered at 200°C. Denotation of chemical compositions are summarised in table 2.

TABLE 2

Chemical composition and designation of sintered materials

Chemical composition	Sintering atmosphere	
	Nitrogen	Hydrogen
Fe-3Mn-0.6C-0.5Mo-0.03Si	A1	A2
Fe-3Mn-0.8C-0.5Mo-0.04Si	B1	B2
Fe-4Mn-0.6C-0.5Mo-0.04Si	C1	C2
Fe-4Mn-0.8C-0.5Mo-0.04Si	D1	D2
Fe-0.5Mo-0.6C	E1	E2
Fe-0.5Mo-0.8C	F1	F2

3. Testing of sintered specimens

Tensile test

The tensile properties were ascertained for as-sintered steels on dogbone tensile specimens according to PN– EN 10002–1 standard. Tensile test was carried out with MTS 810 testing machine at a crosshead speed of 0.5 mm/min. Elongation was measured with a 10 mm MTS 632.13C-23 extensometer. The load applied and strain were recorded continuously throughout the test. The resulting stress-strain curves were analysed to identify the 0.2% offset yield strength ($R_{0.2}$), tensile strength (UTS) and tensile elongation at fracture (A_{tot}). In addition to the tensile and elongation testing, failed specimens underwent metallographic examination. The results of tensile test are presented in tables 3 and 4.

Bend test

Transverse rupture strength (TRS) was determined by three-point bend testing with stress at fracture evaluated used simple beam theory, i.e. assuming elastic behaviour, according to PN–EN ISO 3325 standard on dogbone tensile specimens. The fixture had two support cylinders mounted parallel with the 28.6 mm distance between the centres. The load cylinder was mounted midway between the support cylinders. The testing equipment provided a static condition of loading. The value at which the load suddenly dropped to the first crack was recorded. The transverse rupture strength, in MPa, was calculated from the Navier formula:

$$TRS = 3Fl/2bh^2, [MPa] \quad (1)$$

where: F — is a load, in Newtons', required for structure, measured at the moment of breakdown of the piece; l — is the distance, in mm, between supports; b — is the width, in mm, of the test piece at right angels to its height; h — is the height (thickness), in mm, of the test piece parallel to the direction of the test load application

Although this procedure is only truly applicable to brittle specimens [12, 13], it was used in this study as a routine measure to quickly distinguish between the apparent bend strength of the investigated alloys. The results of bend test are summarised in table 3.

Apparent and cross-sectional hardness

The apparent hardness, as well as cross-sectional hardness was determined by means of Brinell and Vickers hardness tester respectively, according to the PN-EN ISO 6506 and PN–EN ISO 3878. The results of hardness are shown in table 4.

4. Results

Strength properties

The results obtained during investigations six groups of Fe-(Mn)-(Mo)-C steels are summarised in tables 3 and 4. The average green and as-sintered density range was from 6.93 to 7.16 g/cm^3. The initially carbon content was 0.6 wt.-% for mixtures coded B and E and 0.8 wt.-% for the rest of mixtures. As was shown in table 3, after sintering in nitrogen atmosphere only tensile strength of A, B, C, and D steels was lower than after sintering in hydrogen. For the rest group of steels, sintered in hydrogen, recorded UTS values were similar or lower then achieved after sintering in nitrogen. The differences in these values were in the range from 2 to 6%.

Also TRS recorded during the three-point test for all groups of steels was higher for samples sintered in nitrogen, except C steel, where higher TRS value was achieved after sintering in hydrogen. The changes of TRS were in the range from 4.5 to 13%.

When we look at plasticity and hardness of Fe-(Mn)-(Mo) PM steels (table 4), the increase of these properties was achieved after sintering in nitrogen atmosphere. High plasticity and cross-sectional hardness of all steels is connected with the presence of plastic and hard structural constituents existing in the structure after tempering – martensite, retained austenite, bainite and troostite. It can be also pointed out such high, as for this group of PM steels, elongation — up to 2.99% (table 4 — steel A).

TABLE 3

Properties of sintered PM steels — sintering temperature 1220°C

Type of mixture	green density, g/cm^3	as-sintered density, g/cm^3	UTS, MPa	TRS, MPa
A1	7.04	7.04	639	1253
A2	7.05	7.05	659	1164
B1	7.01	7.01	600	1390
B2	7.00	6.99	635	1205
C1	6.93	6.94	535	954
C2	6.94	6.94	564	1092
D1	6.91	6.91	455	1032
D2	6.93	6.93	467	985
E1	7.11	7.11	486	982
E2	7.11	7.12	466	921
F1	7.14	7.16	541	1041
F2	7.16	7.15	512	964

TABLE 4

Plasticity and hardness of sintered PM steels — sintering temperature 1220°C

Type of mixture	$R_{0,2}$ yield strength, MPa	A_{tot}, %	apparent hardness HB	cross-sectional hardness HV_{30}
A1	535	2.99	236	255
A2	453	2.70	252	250
B1	385	2.83	276	312
B2	417	2.88	248	285
C1	385	1.60	276	281
C2	369	1.71	280	301
D1	—	1.10	301	280
D2	384	1.23	272	224
E1	351	2.32	176	133
E2	359	1.97	159	165
F1	383	2.34	183	151
F2	350	2.14	174	163

Microstructure

Microstructure analysis of Fe-(Mn)-(Mo)-C PM steels was carried out on 3% nital etched surfaces using Leica DM 4000 microscope. Bright field as a microscope technique was employed. Working magnification was 1000x.

Fe-3Mn-0.5Mo-0.6C-0.03Si — steel A

After sintering in nitrogen in sintered steels small decarburisation effect was observed (Fig. 2). The structure mainly consists of bainite/martensite regions. Also ferritic and austenitic islands and fine pearlite were observed (Fig. 3). Some slag and oxides were also presented. Sintering in hydrogen caused to increasing decarburisation effect.

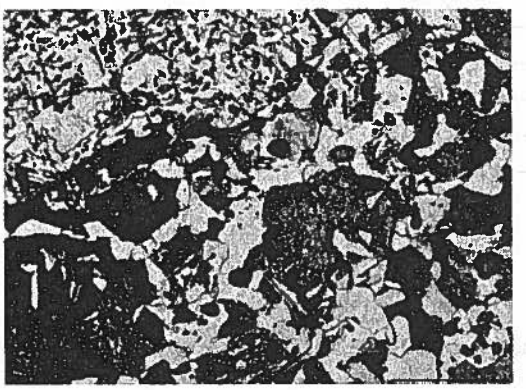

Fig. 2. Microphotograph of steel A; ferritic/pearlitic region near the surface. In the left top corner bainite. (N_2, mag. 1000x)

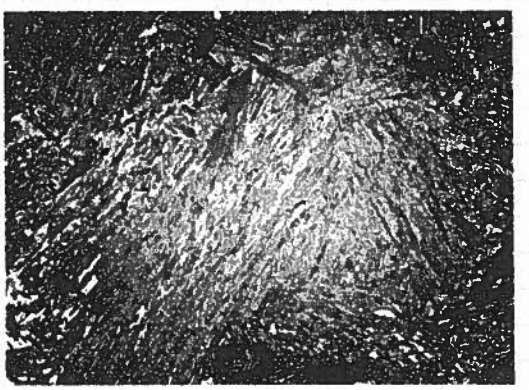

Fig. 3. Microphotographs of steel A; austenitic island (N_2, 1000x)

These ferritic/pearlitic regions are uniformly presented in bainitic matrix. The interior of the specimens consists of bainite, austenite and martensite. Undependable on sintering atmosphere, the observed structures were heterogeneous.

Fe-3Mn-0.8C-0.5Mo-0.04Si — steel B

The steel sintered in nitrogen was characterised by large inhomogeneity of the structure. Near the surface there were sparsely presented ferritic/pearlitic regions. The structure contains mainly tempered martensite, retained austenite and bainite. The small amount of austenitic islands, locate into martensite/austenite or austenite matrix, were also observed. Characteristic spherolitic regions, presented in the structure, are built from troostite, separated from austenite by bainitic regions (Fig. 4). After sintering in hydrogen the structure inhomogeneity was observed. A lot of ferritic/pearlitic islands existed in bainitic matrix are presented near the specimens surface. Martensite and austenite are located alternate with ferritic/pearlitic regions. Oxides and pores were also presented.

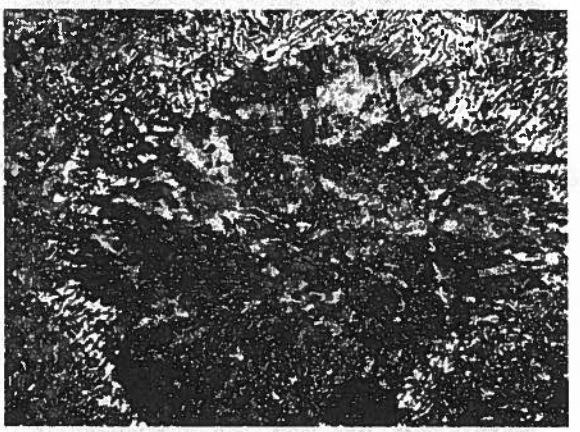

Fig. 4. Microphotograph of steel B; from the middle of spherolite — troosite, bainite and austenite (N_2, 1000x)

Fe-4Mn-0.6C-0.5Mo-0.04Si — steel C

In the samples sintered in nitrogen the predominant structural constituents were martensite and retained austenite; bainite was observed very seldom. Also in the structure characteristic austenite island could be observed as well as lot of slagging, pores and oxides. The other characteristic constituents are austenite rims arounded by martensite, inside which bainite is presented. After sintering in hydrogen, near the surface the thin carbides layer in bainitic matrix existed and was divided by ferritic/pearlitic region. Predominant constituents were martensite and retained austenite, fine pearlite (troostite)

and big bainitic islands with carbide precipitations. Oxides and slag inclusions were also observed.

Fe-4Mn-0.8C-0.5Mo-0.04Si — steel D

After sintering in nitrogen there was no evident decarburisation effect. The structure near the surface was mainly bainitic (Fig. 5);

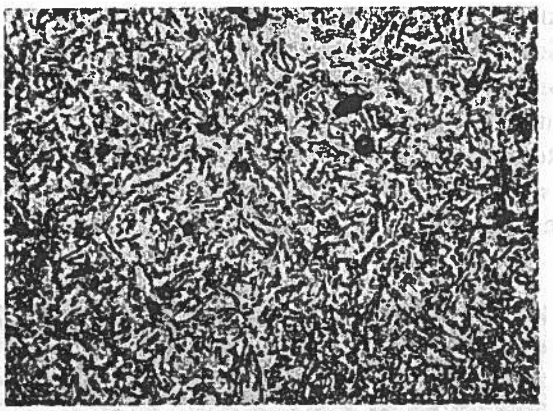

Fig. 5. Microphotographs of steel D; bainitic matrix (N_2, 1000x)

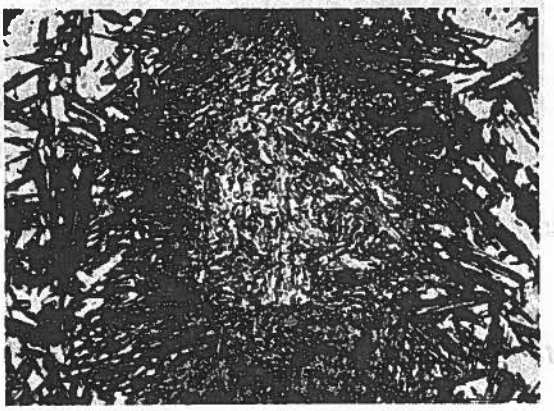

Fig. 6. Microphotographs of steel D; from the middle of the structure — bainite, austenite, martensite (N_2, 1000x)

interior of samples consist of martensite and retained austenite, which sometimes created islands inside which bainite were presented (Fig. 6). The structure is characterised by small inhomogeneity. Sintering in hydrogen had no influence on the decarburisa-

tion effect. In the structure, with small inhomogeneity, the microstructure constituents existed as after sintering in nitrogen.

Fe-0.5Mo-0.6C — steel E

After sintering in nitrogen slightly decarburisation effect was recorded. The structure, with a small inhomogeneity, created pearlite and bainite (Fig. 7). There was no difference in the structure after sintering in hydrogen.

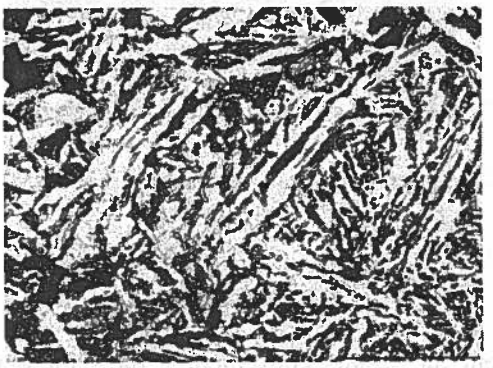

Fig. 7. Microphotographs of steel E; fine pearlite and bainite (N_2, 1000x)

Fe-0.5Mo-0.8C — steel F

Sintering in nitrogen caused to create pearlitic regions. The structure was mainly built from ferrite and fine pearlite (Fig. 8). Also coarse pearlite was grouped in big clusters. In the microstructure the small amount of pores and contaminations were ob-

Fig. 8. Microphotographs of steel F; ferrite and pearlite (N_2, 1000x)

served. After sintering in hydrogen small inhomogeneity of the structure was recorded. The structure mainly consists of pearlite (Fig. 9).

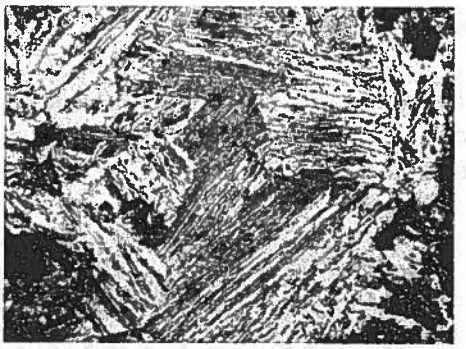

Fig. 9. Microphotographs of steel F; coarse pearlite (N_2, 1000x)

5. Discussion

In order to present the results conveniently, the data were grouped into twelve (A1-F2) categories and the results were presented in tables 3 and 4. These data show the influence of chemical composition and sintering atmosphere on the properties of PM (Mn)-(Mo) steels. The alloys regarded here belong to the group of low alloyed sinter-hardened medium-to-high strength steels, which are used for structural parts in ferrous powder metallurgy. The steels achieved tensile strengths up to 640 MPa and maximum yield strengths of 535 MPa. The highest UTS, TRS, A_{tot}, $R_{0,2}$ yield strength and cross-sectional hardness were achieved for steels coded A2, B1, A1, A1 and B1 respectively. These both groups, A and B, contain 3 wt.- % of manganese, what in combination with molybdenum has been found very effective. Increasing manganese content up to 4 wt.-% decreased the properties of steels. Also shortage of manganese as an alloying element rapidly decreased the properties. There was no clear correlation between density and tensile strength of sintered specimens as well. When these differences are low, mechanical properties mainly depend on the chemical composition.

The TRS/UTS ratio was in the range from 1.77 to 2.31. Considering these results it can be concluded that the samples had good plasticity — although elongation not exceeded 3%.

Properties of examined steels good correspond with their heterogeneous structure. Metallographic observation of the specimens containing manganese and molybdenum revealed complex structure consisting of bainite, martensite and manganese-rich retained austenite. The specimens had also regions of pearlite and molybdenum-rich ferrite. Diagrams presented in figs. 10 and 11 confirm the structural constituents presented in examined steel. After cooling rate 64°C/min, what is equal approx. 1.1°C/s, in the structure hard and non-plastic constituents were presented. When tempering at

200°C was employed, sintered steels achieved good combination of moderate tensile properties and plasticity, what was shown in tables 3 and 4.

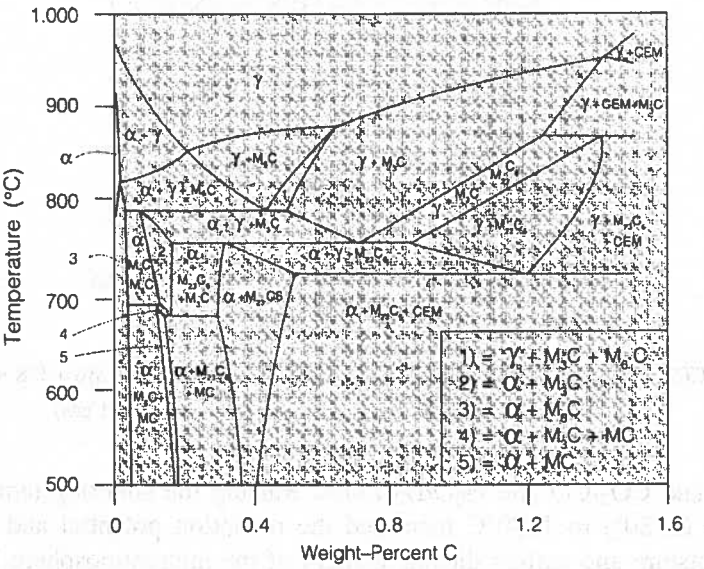

Fig. 10. Phase diagram Astaloy Mo-carbon

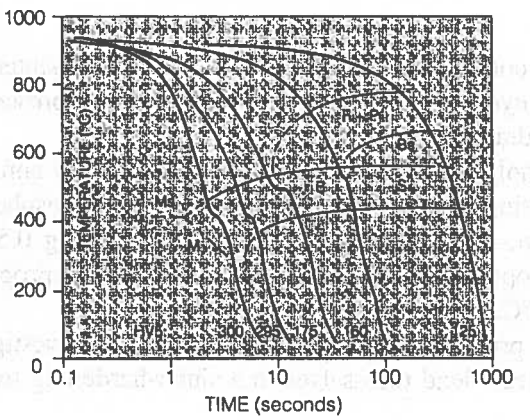

Fig. 11. CCT diagram for cooling rate 1, 10, 50, 97 and 256°C — Astaloy Mo + 0.2 wt.-% of C (austenitizing — 920°C/20min/vaccum; quenching inert gas)

There was no evident difference in properties of these steels sintered in nitrogen or hydrogen atmosphere. When sintering was carried out in semi-closed container might be attributed to the fact that removal of the surface layers of oxides on powder is dependent on the reduction potential of the local microatmosphere. It varies with

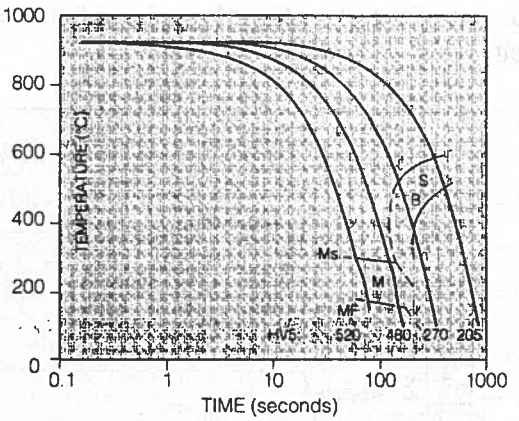

Fig. 12. CCT diagram for cooling rate 1, 2.5, 5 and 10°C — Astaloy Mo + 0.8 wt.-% of C (austenitizing — 920°C/20min/vaccum; quenching inert gas)

temperature and CO_2/CO and H_2O/H_2 ratios. Raising the sintering temperature from conventional (1120°) to 1220°C increased the reduction potential and overcame the effects of moisture and carbon dioxide content of the microatmosphere [14, 15].

6. Conclusions

This study has contributed to show the possibility of sintering Fe-(Mn)-(Mo)-C steels in differ than hydrogen atmosphere. On the basis of present work the following conclusions can be drawn:

1. Manganese — molybdenum structural PM steels display similar mechanical properties after sintering in both nitrogen and hydrogen atmosphere.
2. Addition of 3 wt.-% manganese to PM steel containing 0.5 wt.-% molybdenum has been found optimal with respect to the mechanical properties of the material sintered at 1220°C.
3. The mechanical properties achieved indicate that the investigated manganese-molybdenum PM steels lend themselves to a sinter-hardening treatment.

Acknowledgements

This paper was presented as a poster at PMAsia 2005 Conference and Exhibition, which was held in Shanghai 4-6.04.2005.

The financial support of the Ministry of Scientific Research and Information Technology under the contract no 3T08D 039 27 (AGH-UST contract no 18.25.110.607) is gratefully acknowledged.

REFERENCES

[1] A. Cias, Development and Properties of Fe-Mn-(Mo)-(Cr)-C Sintered Structural Steels. Habilitation Thesis, AGH-UST, Cracow, 2004.
[2] A. Salak, The International Journal of Powder Metallurgy and Powder Technology **16**, 4, 369(1980).
[3] G. Zapf, G. Hoffman, K. Dalal, Powder Metallurgy **18**, 35, 214 (1975).
[4] R.J. Causton, T.M. Cimino, Proc. of International Conference and Exhibition on Powder Metallurgy and Particulate Materials, MPIF, Toronto, Canada 1994.
[5] A. Romański, Optymalizacja Składu Chemicznego i Parametrów Wytwarzania Spiekanych Stali Fe-Mn-Mo- C. Master Thesis, AGH-UST, Cracow 1997.
[6] A. Romański, A. Cias, Inżynieria Materiałowa **4**, XIX, 1175 (1998).
[7] A.S. Wronski et al., Tough, fatigue and wear resistance sintered gear wheels, Final Report on EU Copernicus Contract no ERB CIPA-CT94-0108, European Commission 1998.
[8] S.C. Mitchell, A.S. Wronski, A. Cias, M. Stoytchev, Proc. of PM^{2}TEC International Conference on the „Advances in powder metallurgy and particulate materials", MPIF, Vancouver **2**, 7-129 to 7-144 1999.
[9] R. Keresti, M. Selecká, A. Šalak, Proc. of International Conference DFPM'99, IMR-SAS Kosice, Pieštany, **2**, 108-111 1999.
[10] M. Youseffi, S.C. Mitchell, A.S. Wronski, A. Cias, Powder Metallurgy **43**, 353 (2000).
[11] A. Šalak, M. Selecka, L. Parilak, Proc of European Congress PM2001, EPMA, Nice, 2001.
[12] A. Cias, M. Stoytchev, A.S. Wronski, Proc. of International Conference on Powder Metallurgy and Particulate Materials, MPIF, New Orleans 10-131 to 10-140 2001.
[13] S.C. Mitchell, A.S. Wronski, A. Cias, Inżynieria Materiałowa **5**, XXII, 633 (2001).
[14] A. Cias, S.C. Mitchell, K. Pilch, H. Cias, M. Sulowski, A.S. Wronski, Powder Metallurgy **46**, 2, 165 (2003).
[15] S.C. Mitchell, A.S. Wronski, J. Georgiev, M. Stoytchev, Proc of PM World Congress, EPMA, Vienna 2004.

Received: 5 December 2004.